Heat and Mass Transfer 38 (2002) 705–712 © Springer-Verlag 2001
DOI 10.1007/s002310100266

Thermal optimization on micromachined convective accelerometer

X. B. Luo, Z. X. Li, Z. Y. Guo, Y. J. Yang

Abstract A kind of micromachined convective accelerometer without solid proof mass is numerically and experimentally studied in this paper. The accelerometer consists of a micro heater and two temperature sensors which measure the temperature difference between two symmetrical positions on both sides of the micro heater. The temperature difference is caused by free convection due to acceleration. Thermal optimization on the accelerometer is conducted based on numerical simulation. Three important indexes of the accelerometer, linearity, sensitivity and frequency response are discussed respectively. The results show that linearity relates with the non-dimensional number Gr, only when Gr is in the range from 10^{-2} to 10^{3}, good linearity can be achieved. The optimum sensor position for high sensitivity and good linearity is near at $x/D = 0.3$. An increase of heating power or cavity size leads to an increase in the sensitivity. The working media that has small density ρ and large thermal diffusivity α is favorable for fast frequency response, the one having large density ρ and small kinematic viscosity υ will be advantageous for high sensitivity. Experimental tests prove that the optimized convective accelerometer has good linearity, high sensitivity and preferable frequency response.

List of symbols

a	acceleration
c_p	specific heat
d	cavity depth
D	half of cavity length
Gr	Grashof number
k	thermal conductivity
L	heater width
p	pressure
Pr	Prandtl number
R	ideal gas constant
Ra	Rayleigh number
t	time
T	temperature
T_w	heater surface temperature
u	velocity
x	the distance between sensor and heater
ΔT	temperature difference between heater and environment

Greek symbols

α	thermal diffusivity
β	bulk expansion coefficient
δT	temperature difference of two sensor
μ	dynamic viscosity
υ	kinematic viscosity
ρ	density
ρ_0	density at environment temperature

Received on 9 March 2001 / Published online: 29 November 2001

X. B. Luo, Z. X. Li (✉), Z. Y. Guo
Department of Engineering Mechanics
Tsinghua University, Beijing, 100084, China

Y. J. Yang
Hebei Semiconductor Research Institute
Shijiazhuang, 050051, China

This work was supported by the National Natural Science Foundation of China (Grant No 59995550-2), the authors gratefully acknowledge the financial support.

1 Introduction

Demands for low-cost and high performance accelerometers have been increasing in many fields including automobile industry, navigation systems, military industry, robotics systems [1] and fundamental physics experiments [2]. Consequently, many efforts have been made in developing micromachined accelerometers in recent years to meet the low-cost requirements [3–8].

So far, common designs of micromachined accelerometers involve solid proof mass, which is allowed to move under accelerating conditions. However, for micromachined accelerometers, the inertial forces that are detected as the measures of accelerations are very small because of the tiny proof mass, so it is difficult to achieve high sensitivity [9]. In addition, the existence of the proof mass brings some disadvantages to the accelerometers, such as, low resistance ability to shock, being difficult to sense the motion of the proof mass accurately and so on [8].

Recently, a novel concept and device structure for measuring acceleration were developed by Dao et al. [10], operation of the accelerometer is based on free convection of a tiny hot air bubble in an enclosed chamber. It doesn't require solid proof mass and is compact, lightweight, inexpensive to manufacture and sensitive to small accelerations. Leung et al. [11] reported the implementation of the device structure by bulk silicon fabrication, the test shows that the device has low cost and can gain high sensitivity, which make it a very competitive commercial device. Milanovic et al. [12] fabricated two kinds of the convective accelerometers, thermopile and thermistor types in stan-

dard IC technology. Their accelerometers exhibited some significant advantages such as low cost, miniaturization, integration and good frequency response.

Since operation of the convective accelerometer is based on free convection, the key to upgrade the performance of accelerometer and actualize its potential is to improve the convection in the device. As Leung et al. [11] and Milanovic et al. [12] presented in their papers, work should be under way to characterize them in various conditions to achieve higher performance. In this paper, thermal analyses are conducted to optimize the convective accelerometer by numerical simulations. Three important indexes of the accelerometer, linearity, sensitivity and frequency response are discussed respectively. Based on the thermal analyses, one kind of optimized convective accelerometer is presented. The experimental measurements on the device prove that it has better linearity, higher sensitivity and more preferable frequency response than some other reported convective accelerometers.

2
Device structure and basic principle

Figure 1 shows the device structure of a micromachined convective accelerometer. It includes an electric heater and two temperature sensors mounted within a sealed enclosure containing a kind of gas. The sealed enclosure aims to prevent environmental air flow from disturbing the device's operation. The temperature sensors are positioned symmetrically on both sides of the microheater. The microheater is used to heat the gas and therefore to create a free convection when acceleration is applied to the gas. The heater temperature and gas temperature distributions along the X axis are illustrated in Fig. 2. In the case of no acceleration or the acceleration normal to the X axis of accelerometer, the flow pattern and gas temperature distribution are symmetrical as the dash lines show due to the symmetric locations of two temperature sensors. As a result, no temperature difference exists between two temperature sensors no matter how high the heater temperature is. As long as the acceleration at X axis appears, the free convection along X axis is produced or the gravity induced convection is skewed. This must lead to the asymmetric distributions of gas temperature shown by the solid lines in Fig. 2. Consequently, the temperature difference between two sensor positions becomes nonzero. Apparently, the temperature difference between two sensors increases with increasing the acceleration at the X axis. By measuring the temperature difference, the acceleration information can be acquired.

3
Governing equations and numerical simulations

Since the dimensions of the micromachined convective accelerometer and the gas velocity are small, the gas flow in the accelerometer is usually laminar. The free convection is caused by the body force due to acceleration and spatial density variation resulted from the spatial temperature change in the enclosure. The governing equations for free convection are as follows:

Equation of continuity:

$$\nabla \cdot u = 0 \tag{1}$$

Equation of momentum:

$$\rho u \cdot \nabla u = -\nabla p + \mu \nabla^2 u + \rho a \tag{2}$$

Equation of energy:

$$\rho c_p u \cdot \nabla T = k \nabla^2 T \tag{3}$$

Equation of state:

$$\rho = p/RT \tag{4}$$

Numerical simulations were conducted. The commercial code named STAR-CD was adopted for the simulations. In the computations, μ, c_p, k were given the constant values at the average of the heater and environment temperatures.

For the device shown in Fig. 1, because the ratio of the lengths of heater and temperature sensors to their widths and heights is very large, the two dimensional model can be adopted. Figure 3 illustrates the convective accelerometer model we simulated. For simplicity, both cavity wall and heater are regarded as isothermal boundaries. In the computations, different grid distributions are adopted at different model size, fine grid distributions are adopted in the region near heater, direction of acceleration a is towards left.

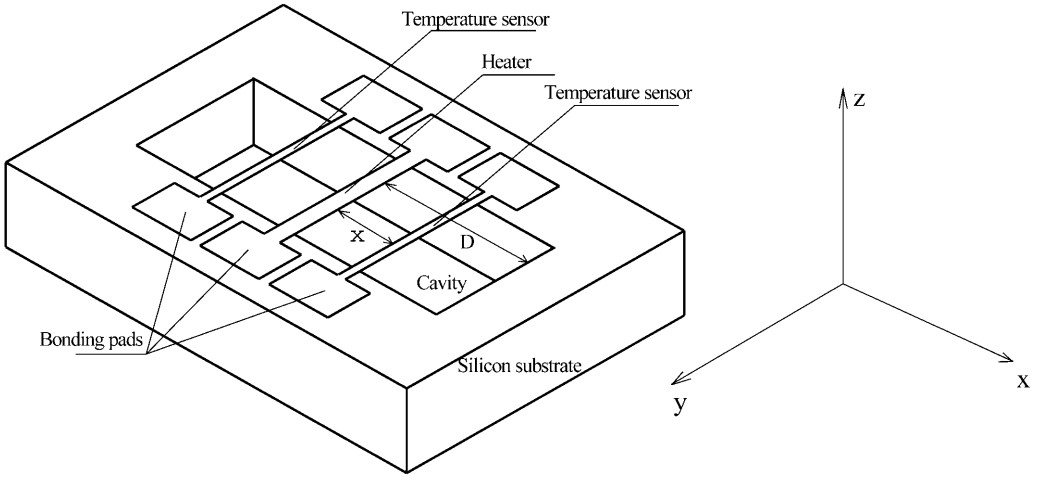

Fig. 1. Device structure of a micromachined convective accelerometer

The following numerical simulations and analyses are made starting from an accelerometer prototype having such characteristics: the temperature of heater surface is 973 K, the cavity size is 960 × 100 μm, the gas media is air.

4 Thermal optimization

Sensitivity, linearity and response frequency are three of the most important performance indexes for accelerometers. Good linearity, high sensitivity and fast frequency response are favorable for their application. As for convective accelerometers, according to the preceding principle introduction, good linearity requires that the temperature difference between two sensors is magnificently linear with the exerted acceleration. High sensitivity means large temperature difference at a given acceleration, that is, the larger the temperature difference, the higher is the sensitivity. Fast frequency response demands short thermal and flow inertia time when accelerometer is subjected to a different acceleration.

Obviously, the above three indexes are dependent upon the coupled heat and mass transfer in accelerometer cavity, thereby conducting thermal optimization before design and fabrication will be helpful for the performance improvement of the convective accelerometer.

4.1 Linearity analysis

Two dimensionless parameters, Grashof number Gr, Prandtl number Pr, govern the free convection:

$$\mathrm{Gr} = \frac{a\beta\Delta T L^3}{\upsilon^2} \tag{5}$$

$$\mathrm{Pr} = \frac{\upsilon}{\alpha} \tag{6}$$

Prandtl number is decided by filled gas in the convective accelerometer, thus for an accelerometer that gas media is given, the flow and heat transfer in it are determined by the Grashof number, which implies that the temperature difference between the two sensors is also decided by the Grashof number. In fact, the convective accelerometer is given in a certain application, the parameters in the definition of Grashof number such as β, ΔT, L, υ will be given, thereby the Grashof number is just proportional to acceleration based on Eq. (5). So, the dependence of the temperature difference on Grashof number represents the relation of the temperature difference with acceleration, which is also the base of the following linearity discussion. Figure 4 depicts the dependence of the temperature difference on Grashof number.

In Fig. 4, both abscissa and ordinate adopt logarithmic coordinates, the ordinate δT represents the temperature difference between two sensors. It can be seen from Fig. 4 that for Grashof number, in the range of larger than 10^{-2} and smaller than 10^3, the temperature difference is almost linear with Grashof number. That is to say, in the above range for Gr, the output of convective accelerometer is linear with acceleration. Why does the linear relation exist in this region? It can be explained as follows. There are three forces, inertial force, viscous force and buoyancy force, which govern the natural convection. For the natural convection with large Grashof number, which may be resulted from large scale, large temperature or large acceleration, the inertial force term is not too small to be

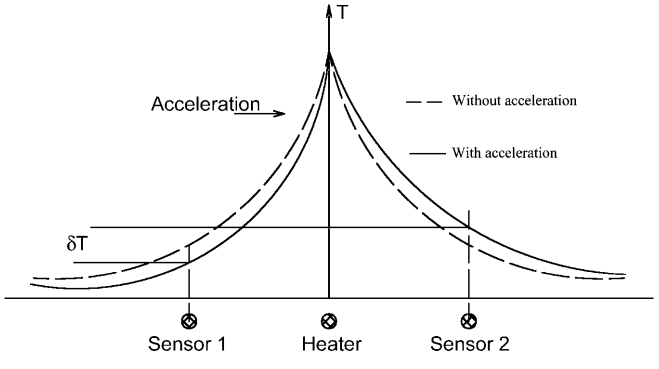

Fig. 2. Symmetrical temperature distribution generate by the central heater is disturbed by applied acceleration

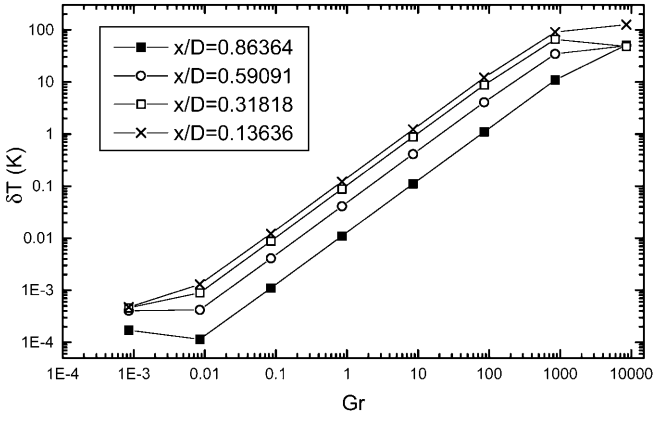

Fig. 4. Temperature difference versus Gr

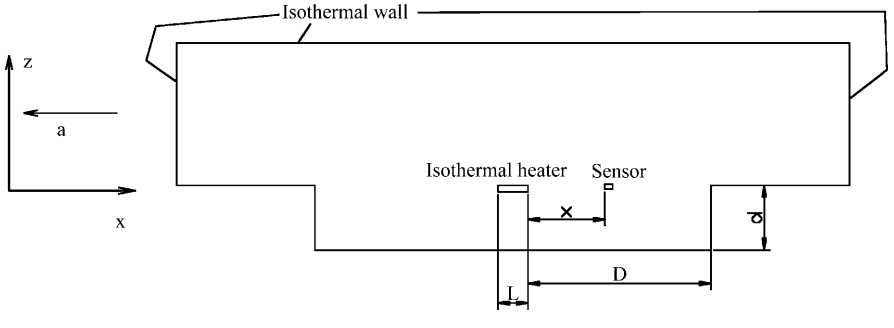

Fig. 3. Schematic of simulated convective accelerometer

neglected compared to viscous force, thus the governing equations show non-linearity characteristics, consequently, the flow and heat transfer in the accelerometer exhibit non-linearity. For the natural convection with small Grashof number, heat conduction in the convective accelerometer overwhelmingly prevails over the convection, thereby the non-linearity in small Gr condition may be contributed to the increasing influence of the heat conduction where the inertial force is very small compared to viscous force. Only in the range of Gr larger than 10^{-2} and smaller than 10^3, the convective accelerometer exhibits a performance of output linear with acceleration. The reason is that the natural convection in the accelerometer is governed by both viscous force and buoyancy force, the inside heat conduction is not too strong compared to the natural convection.

The effect of sensor position on the linearity of convective accelerometer is also simulated, the result is illustrated in Fig. 5. The abscissa x/D denotes the non-dimensional position of the temperature sensor, the ordinate denotes the linearity error, which is defined as the real numerical results divided by the value obtained from the fitting line. It is noted from Fig. 5 that the linearity error is smallest when x/D ranging from 0.3 to 0.7, where it is around 0.05%. When the sensor is positioned at other position, it can increase to 0.5%, so suitable sensor position will be advantageous to the linearity improvement.

4.2 Sensitivity analysis

It is necessary to understand which factors affect the sensitivity (temperature difference) of the convective accelerometer. First of all, the strength of convection has significant impact to it. From Eqs. (5) and (6), it is found that heating power and gas properties influence the convection strength. In addition, the cavity dimensions and boundary conditions are of influence on free convection in an enclosure, including flow pattern and convection strength. In present computations, the cavity height is comparable with heater width, thus the effect of cavity size should also be considered. Besides the above three factors, the temperature difference between two sensors may vary remarkably for different location of sensors, therefore, the location effect of the temperature sensor on sensitivity must be taken into consideration. In order to upgrade the accelerometer sensitivity, the above-mentioned four factors will be examined in detail.

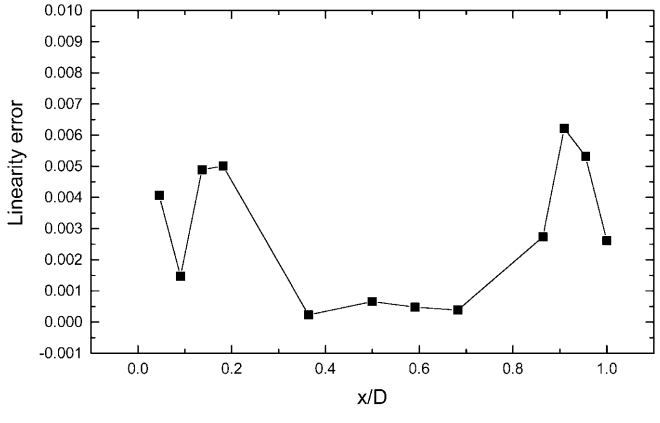

Fig. 5. Linearity error versus the sensor position

Effect of heating power

In view of that heating power produces the convection and the consequent temperature difference between sensors, the effect of heater temperature should be discussed in present computations. Flow and temperature fields have been simulated for four cases of heater surface temperatures of 423, 573, 773 and 973 K at given cavity size, gas media (air) and acceleration ($10g$) as shown in Fig. 6. The corresponding temperature differences of two sensors for different sensor locations are given in Fig. 7, it is evident from Fig. 7 that the temperature difference of two sensors and hence the sensitivity of the accelerometer increases monotonously with increasing heater temperature.

Effect of sensor position

Assuming that two sensors are located far from the heater, their temperature difference will obviously be very small. On the contrary, if they are located very near to the heater, the temperature difference of two sensors will approach zero. So, it can be expected that there must be a maximum in temperature difference of sensors at some specific position. Numerical results of the temperature difference confirm this analysis. It can be seen from Fig. 8 that in all four heater temperature cases, the sensor has an optimum position, where the temperature difference between two sensors reaches to its maximum. It means that when the sensor is located at this position, the accelerometer will be of highest sensitivity, while it is worthy noting that the

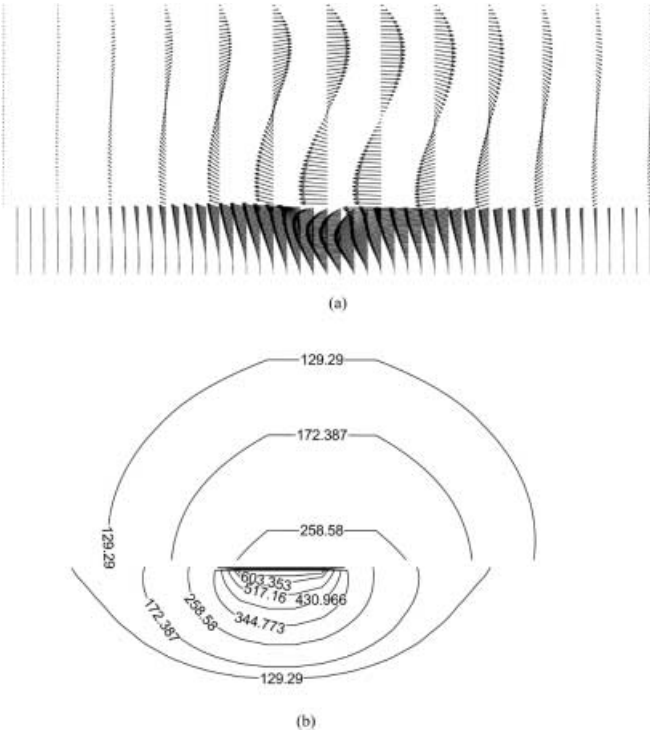

Fig. 6a, b. Simulation results at heater temperature of 973 K **a** velocity distribution, **b** temperature distribution

optimum position is nearly the same in all four cases, which is around $x/D = 0.2$. Apart from the optimum position, the temperature difference measured by two sensors will decline.

Effect of cavity size

The numerical simulations of the variation of temperature difference between two temperature sensors versus cavity size is illustrated in Fig. 9 for the heater temperature at 973 K and the acceleration at 10*g*. It is clear that the temperature difference measured by the two temperature sensors significantly increases with increasing cavity size. This is because the distance between the heater and the bottom wall, *d*, is of the same order of magnitude as the heater width and the consequent space below heater is too small so that free convection is considerably suppressed and the temperature difference between two sensors reduces. Evidence for this explanation can be found in Fig. 10 where the convection strength in the lower part of cavity is much stronger for $d = 250$ μm than that for $d = 100$ μm. However, we also note in computations that when the lower part of cavity size is large enough, for example, the cavity height is 10 time larger than heater width, further increase of cavity size will be of no use for sensitivity. It is also found from Fig. 9 that the optimum position of temperature sensor for sensitivity is around $x/D = 0.2$, which is same as that in different heater temperature cases.

Effect of gas media

The convective accelerometers filled up with different gases have been numerically studied respectively. The corresponding results for gas, air, nitrogen, carbon dioxide and hydrogen are shown in Fig. 11. It can be seen that the sensitivity is the highest when carbon dioxide is filled in the cavity, the convective accelerometers using nitrogen and air as medium nearly have same sensitivity, while the sensitivity for hydrogen as medium is extremely small. The

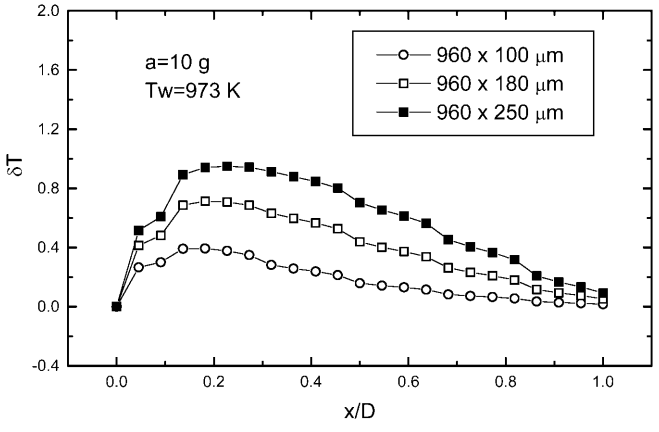

Fig. 9. Dependence of the temperature difference on the sensor location with cavity size as parameter

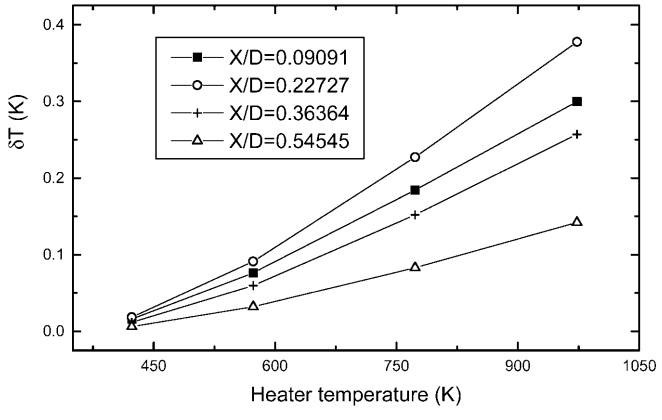

Fig. 7. Dependence of the temperature difference on the heater temperature with different sensor location as parameters

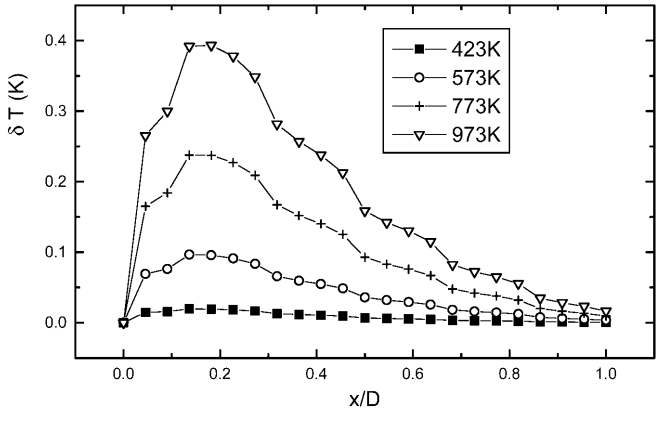

Fig. 8. Dependence of the temperature difference on the sensor location with heater temperature as parameter

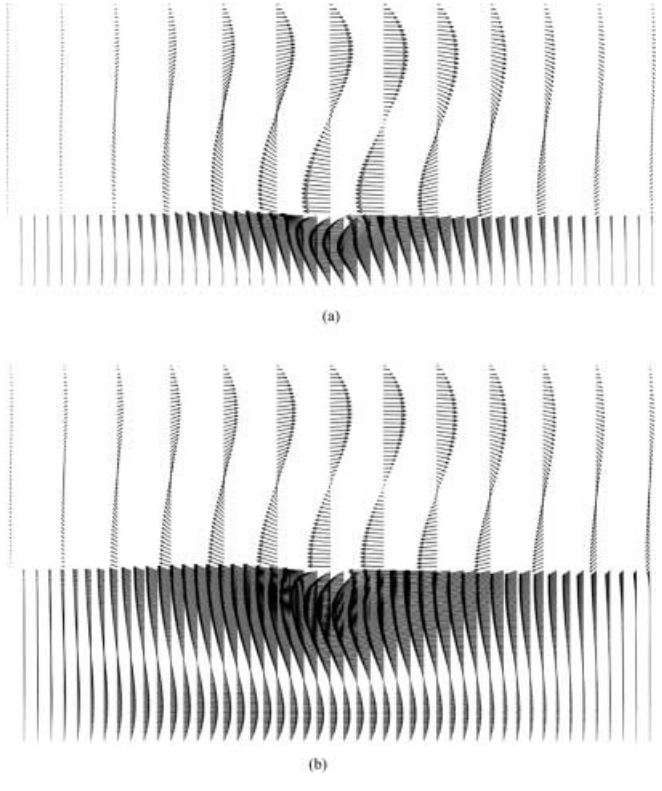

Fig. 10a, b. Velocity distribution for different cavity size **a** 960 × 100 μm, **b** 960 × 250 μm

reasons for these should be attributed to the property difference between different gases. The strength of free convection is usually characterized by Rayleigh number, a product of Grashof number and Prandtl numbers. In other words, strong free convection corresponds to large value of Rayleigh number,

$$\mathrm{Ra} = \mathrm{Gr}\ \mathrm{Pr} = \frac{\beta a \Delta T L^3}{\upsilon \alpha} = \frac{c_p \rho^2 \beta a \Delta T L^3}{\mu k} \qquad (7)$$

Various properties for different gases at 650 K are listed in Table 1. It can be seen that the bulk expansion coefficient, β, is basically independent of kind of gas, the Rayleigh number, hence, depends on the product of dynamical viscosity and thermal diffusivity for the given cavity, acceleration and temperature difference of heater and environment. The product of dynamical viscosity and thermal diffusivity for hydrogen is very large and the corresponding Rayleigh number is very small, the product of υ and α for carbon dioxide is the smallest among four gases and the Rayleigh number is the largest and three times as large as air or nitrogen. These are why the temperature difference for different gases in Fig. 11 is extremely different. These difference are caused by density variation for different gases from Eq. (7), while variation of c_p, k, μ are not remarkable for different gases except for hydrogen as indicated in Table 1. After all, free convection of the high density gas, for instance, CO_2, is of high Rayleigh number and results in the high sensitivity for accelerometers.

In Fig. 11, we also find that optimum position of temperature sensor, as shown in aforementioned computation cases, is around $x/D = 0.2$.

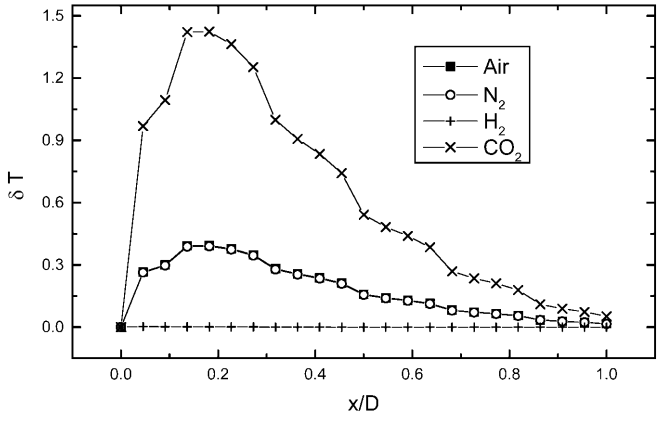

Fig. 11. Temperature difference between two sensors with different working gas

4.3 Frequency response

Frequency response is involved in the transient behavior of the cavity fluid as the accelerometer is instantaneously accelerated. Providing that accelerometer is subjected to a different acceleration suddenly, immediately after $t = 0$, the flow pattern and thermal balance in accelerometer cavity will change. As t increases, the effect of thermal and flow inertial decreases in importance. There comes a final time that the flow and heat transfer along the heater wall reach a steady state, which characterize by a energy balance between the heat conducted from the heater and the enthalpy carried away by the buoyant layer, a momentum balance between buoyancy and viscous diffusion. Such a time represents the response frequency of convective accelerometer. It is mainly decided by the gas properties. The key properties are thermal diffusivity and density. Larger the thermal diffusivity and smaller the density, less the time will be spent, so large thermal diffusivity and small density will be favorable for high response frequency. Since hydrogen has large thermal diffusivity and small density, although its sensitivity is very low, its response frequency will be high.

5 Design consideration

As for design of the convective accelerometer, good linearity should be considered firstly. According to the preceding analyses, Gr number should be assured in the range from 10^{-2} to 10^3, that is to say, heater width L, heating power should be chosen carefully. Since sensor position has influence on both linearity and sensitivity, combining with aforementioned discussions, the position that is around $x/D = 0.3$ will be favorable for achieving good linearity and high sensitivity synchronously in application. To increase the sensitivity, the design that has large heater width and cavity size should be adopted, high heating power can be inputted providing that the tradeoff between energy consuming and sensitivity is taken into account. As regards the working media, the gas that has small density ρ and large thermal diffusivity α is favorable for fast frequency response, the one having large density ρ and small kinematic viscosity υ will be advantageous for high sensitivity. Thereby, when selecting gas media to fill the convective accelerometers, the application requirement on sensitivity and frequency response should be weighed.

6 Experimental test

A kind of micromachined convective accelerometer is fabricated by bulk-silicon technology based on the thermal optimization. The heater width is 80 μm, the height is

Table 1. Thermal physical properties of four kinds of gas medium at temperature 650 K

Gas medium	β (1/K)	ρ (kg/m^3)	c_p (kJ/kg · K)	$\mu \times 10^5$ (kg/m · s)	$\upsilon \times 10^6$ (m^2/s)	$\alpha \times 10^4$ (m^2/s)	k (W/m · K)
Air	0.0015	0.5425	1.064	3.22	59.9	0.839	0.0484
Nitrogen	0.0015	0.5281	1.085	3.12	59.66	0.823	0.0467
Hydrogen	0.0015	0.0391	14.57	1.51	386.19	5.70	0.325
Carbon dioxide	0.0015	0.8303	1.10	2.88	35.05	0.49	0.0444

2 μm, the cavity size is 3000 μm (length) × 2000 μm (width) × 250 μm (depth), the sensor position is near at $x/D = 0.34$.

The accelerometer is measured under two kinds of application conditions. Firstly, it is tested from $-g$ to g under gravitation by rotating of the sensitivity axis with respect to the earth gravitational field. Figure 12 illustrates the linearity of the accelerometer under gravitation. It shows a very good fit with the expected linear trend. The linearity error is smaller than 0.35%. For a comparison, the non-linear coefficient of the accelerometer in Ref. [11] under gravitation is obviously larger than 1% at the 1g point and that of the device in Ref. [12] is 0.5%.

The device is also measured on a vibration shaker with acceleration range from 0g to 10g and frequency from 0 to 200 Hz. Figure 13 shows that the device has good linearity in the range from 0g to 10g at 45 Hz. The linearity error is larger than that measured under gravitation, which reaches 2%. It is noted from Fig. 13 that the sensitivity of the optimized accelerometer is 600 μV/g for operating power of 87 mW. For a comparison, the sensitivity of the accelerometer in Ref. [12] is 146 μV/g for operating power of 430 mW, the linearity error in acceleration range from 0g to 7g is 2%. Owing to the absence of relative comparable data, here the comparison with that in Ref. [11] can not be carried out.

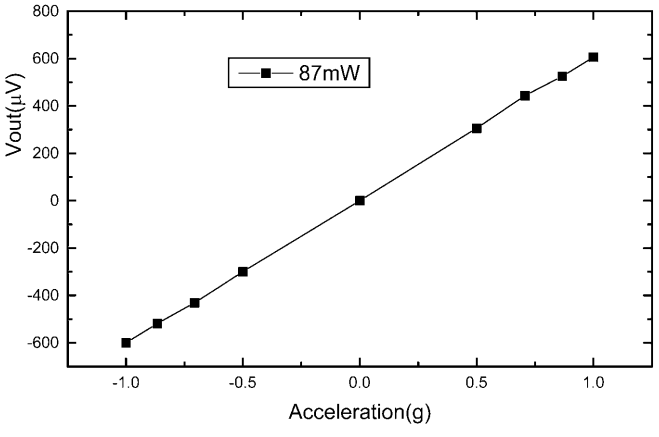

Fig. 12. Linearity of the optimized accelerometer at 87 mW under gravitation

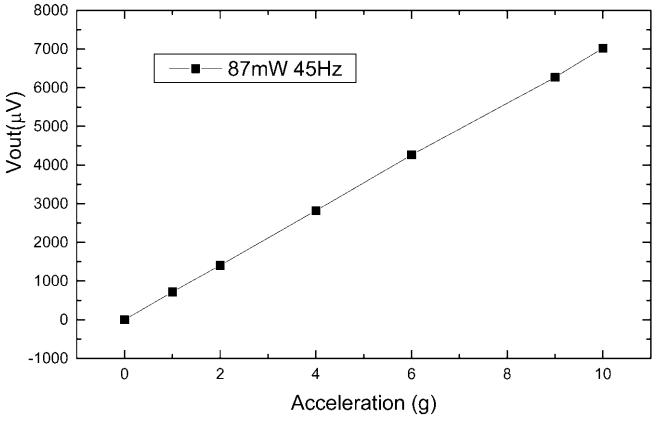

Fig. 13. Measured performance of the accelerometer at 87 mW from 0g to 10g

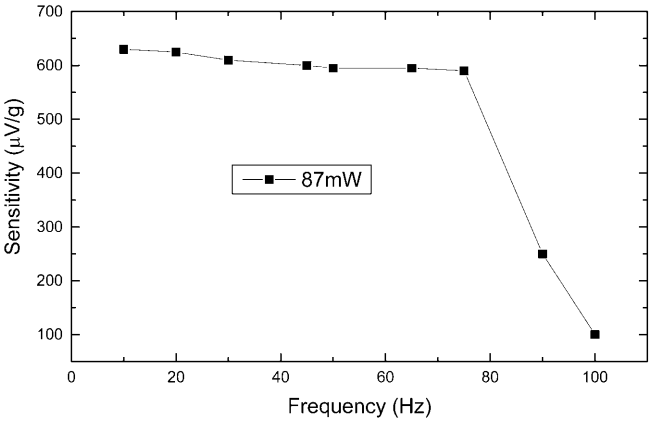

Fig. 14. Measured frequency responses

The frequency response of the device is shown in Fig. 14. It is noted that the frequency response is flat up to about 75 Hz, where the sensitivity decreases substantially. The response frequency is larger than that in Ref. [11], in which it is 20 Hz. However, compared with the response frequency numbered 300 Hz in Ref. [12], it is much smaller. The main reason for this may contributes to the fabrication method and the accelerometer size. In our present work, same as that in Ref. [11], customary bulk-silicon fabrication is adopted, the accelerometer size including cavity size is larger than that in Ref. [12], in which standard integrated circuits technology was employed. According to foregoing optimization analysis, the frequency characteristics of the present accelerometer can not be satisfactory as that in Ref. [12].

7 Conclusions

In this paper, thermal optimization on micromachined convective accelerometers is numerically studied. Simulation results show that the output of the convective accelerometer is linear with Grashof number when the range of Gr is smaller than 10^3 and larger than 10^{-2}. The temperature sensor position ranging from 0.2D to 0.7D will assure the accelerometer having a good linearity. By considering linearity and sensitivity, the temperature sensor positioned at around $x/D = 0.3$ will be favorable for achieving a good linearity and a high sensitivity synchronously. The heater surface temperature, heat width should be carefully chosen in the design. An increase of heating power or cavity size leads to an increase in the sensitivity. The working media that has small density ρ and large thermal diffusivity α is favorable for fast frequency response, the one having large density ρ and small kinematic viscosity υ will be advantageous for high sensitivity. Based on the optimization analysis, a kind of micromachined convective accelerometer is experimentally tested. The experimental results demonstrate that the linearity error of the accelerometer is smaller than 0.35% under natural gravity and smaller than 2% in the case of acceleration ranging from 0g to 10g ($g = 9.81$ m/s^2). A sensitivity of 600 μV/g is measured for

operating power of 87 mW. Both linearity and sensitivity of the accelerometer are better than those reported in literatures.

References

1. **Cimoo Song; Meenam Shinn** (1998) Commercial vision of silicon-based inertial sensors. Sensors and Actuators A66: 231–266
2. **Iafolla V; Mandiello A; Nozzoli S** (2000) The high sensitivity Italian spring accelerometer for fundamental physics in space. Adv Space Res 25(6): 1241–1244
3. **Yazdi N; Ayazi F; Najafi K** (1998) Micromachined inertial sensors. Proc IEEE 86(8): 1640–1659
4. **Kim KH; Ko JS; Cho YH; Lee K; Kwak BM** (1995) A skew-symmetric cantilever accelerometer for automotive airbag applications. Sensors and Actuators A50: 121–126
5. **Nemirovsky Y; Nemirovsky A; Muralt P; Setter N** (1996) Design of a novel thin film piezoelectric accelerometer. Sensors and Actuators A56: 239–249
6. **Kubena RL; Atkinson GM; Robinson WP; Stratton FP** (1996) A new miniaturized surface micromachined tunneling accelerometer. IEEE Electron Device Letter 17(6): 306–308
7. **Dauderstadt UA; De vries PHS; Hiratsuka R; Sarro PM** (1995) Silicon accelerometer based on thermopiles. Sensors and Actuators A46–47: 201–204
8. **Bochobza-Degani O; Seter DJ; Socher E; Nemirovsky Y** (2000) Comparative study of novel micromachined accelerometers employing MIDOS. Sensors and Actuators A80: 91–99
9. **Lim MK; Du H; Su C; Jin WL** (1999) A micromachined piezoresistive accelerometer with high sensitivity: design and modelling. Microelectronic Eng 49: 263–272
10. **Dao R; Morgan DE; Kries HH; Bachelder DM** (1996) Convective accelerometer and inclinometer. US Patent 5581034
11. **Leung AM; Jones J; Czyzewska E; Chen J; Pascal M** (1997) Micromachined accelerometer with no proof mass. Technical Digest of Int Electron Device Meeting, 899–902
12. **Milanovic V; et al** (2000) Micromachined convective accelerometers in standard integrated circuits technology. Appl Phys Lett 76(4): 508–510